Journal of Hydroscience and Hydraulic Engineering
Vol. 20, No.1 May, 2002, 167-178

A FREE-CONVECTION PLUME GENERATED ON A SLOPING BOUNDARY WITH CONSTANT BUOYANCY

By

K.MICHIOKU, I.FUJITA

Kobe University, Nada, Kobe, JAPAN

T.TAKAHASHI

Fukken Chosa Sekkei Co. Ltd., Hiroshima, JAPAN

and

K.YABUMOTO

MYCAL Co. Ltd., JAPAN

SYNOPSIS

Momentum and scalar transports were investigated in a flow system where an inclined plate is heated up with a constant temperature to generate a thermal plume on a sloping boundary. The plume is a free convection in that there is no external mass and momentum supply. The purpose of the system is to simulate an anaerobic reservoir hypolimnion on a sloping bed where heavy solutes such as ionic metals and inorganic nutrients released from the bed flow down the sloping boundary toward the lower region of lake bottom. Temperature and velocity profiles were measured by using thermocouples and a particle-tracking velocimetry, respectively. By means of flow visualization using fine tracer particles and a sophisticated PTV algorithm the velocity measurement proved to be accurate even in such a sluggish density current. A theoretical analysis was made to obtain solutions for flow and buoyancy fields assuming the flow to have a self-similar structure along the longitudinal direction. The theory and experiments agreed closely in respect to velocity and buoyancy profiles as well as to the longitudinal evolution of the plume. The flow analysis is an effective method for estimating transport of water quality caused by biochemical reaction in the anaerobic benthic layer.

INTRODUCTION

In the hypolimnion of eutrophic lakes and reservoirs, water is significantly polluted above the bed due to the release of inorganic nutrients, ionic metals and dissolved organic matters from the sediments. The released components increase salinity and thus increase fluid density, which make the contaminated water denser and heavier than the ambient water. On a sloping bed in lakes and reservoirs of steep geomorphology, the heavy polluted water produced by such biochemical reactions slides down to the lake bottom (1). This process must make contamination of hypolimnetic water more serious. An in-situ measurement of the plume is not feasible, since the fluid motions must be too sluggish and thin to be measured. Therefore, experimental and theoretical methods are the only way of evaluating scalar transport due to the plume. A simplified plume model is devised in this study in order to investigate its hydrodynamics.

The system is a thermal plume that is generated by heating up an inclined plate with a constant temperature. A steady two-dimensional thermal plume develops along the sloping bed. The plume is equivalent in the hydrodynamic sense to a solute plume occurring in a prototype reservoir. The dynamic

similarity between the two plume systems is assured by interpreting density anomaly due to temperature to the one due to solute concentration. An experiment was carried out under various conditions of boundary temperature and sloping angle. Velocity and temperature profiles are measured by means of a particle tracking velocimetry PTV and thermocouples, respectively. In order to examine plume dynamics, a theoretical model is developed assuming a self-similar flow structure. Satisfactory agreement between the experiment and the theory is obtained in respect to velocity and temperature profiles. An investigation is made of how the plume properties such as transport rate, specific buoyancy, longitudinal layer development, etc. depend on the sloping angle and the bed surface temperature. Our analysis enables us to evaluate transport rate due to solute-components release from anaerobic sediments on a hypolimnetic sloping bed.

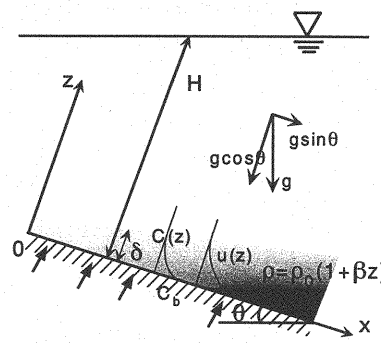

Fig.1 A coordinate system.

ANALYSIS

Governing Equations and Boundary Conditions

Consider a steady two-dimensional plume developed along a sloping boundary as illustrated in Figure 1. Suppose a solute component is released from the sloping boundary along which the solute concentration is uniform and constant. Let the concentration profile be $C(x, z)$. Space coordinates (x, z) are taken in directions along and perpendicular to the boundary, respectively. Buoyancy $B(x, z)$ is defined by $B=\beta gC$, where β is a coefficient relating concentration and density difference and g is the gravitational acceleration. An inclined plume is driven by the density difference between the bed surface and the ambient fluid. Schlichting analyzed a plume along a heated vertical wall (2), while the present analysis investigates a general case of a plume on a wall plate with arbitrary sloping angle θ. Therefore, the Schlichting's analysis corresponds to a special case of $\theta=90^\circ$.

Assuming hydrostatic pressure and applying the approximations of boundary-layer and Boussinesq, equations of continuity, momentum and concentration conservations are written as follows (3):

$$\frac{\partial u}{\partial x}+\frac{\partial w}{\partial z}=0 \tag{1}$$

$$u\frac{\partial u}{\partial x}+w\frac{\partial u}{\partial z}=\underbrace{\beta Cg\sin\theta}_{[G1]}-\underbrace{\frac{\partial}{\partial x}\int_z^\infty \beta Cg\cos\theta dz}_{[G2]}+\nu\frac{\partial^2 u}{\partial z^2} \tag{2}$$

$$u\frac{\partial C}{\partial x}+w\frac{\partial C}{\partial z}=\kappa_C\frac{\partial^2 C}{\partial z^2} \tag{3}$$

where, (u, w) represent flow velocity components in the x and z directions and p is pressure. ν and κ_C are kinematic viscosity and molecular diffusivity of solute substance, respectively.

Boundary conditions at the bed surface $z=0$ is given by

$$u=w=0, \quad C(0)=C_b \quad . \tag{4}$$

Conditions at the uppermost boundary, $z=\infty$, are

$$u=0, \quad C(\infty)=0 \quad . \tag{5}$$

Self-Similar Flow Analysis

Assuming a self-similar flow structure commonly used in jet and plume analyses (see Schlichting (2), Fukushima (4), for example) , the following variable and functions are defined.

$$\eta = azx^{-l}, \quad \psi = bx^{m}F(\eta), \quad C = ex^{n}G(\eta) \tag{6}$$

Here, η is a new dependent variable and $\psi(x, z)$ is a stream function. $F(\eta)$ and $G(\eta)$ are unknown functions in dimensionless forms which respectively correspond to ψ and C. (a, b, e, l, m, n) are undetermined constants.

The following relationships are found by substituting Eq.(6) into Eqs.(1)-(5).

$$m+n-l-1=n-2l, \quad 2m-2l-1=n=l+n-1=m-3l, \quad n=0 \tag{7}$$

They are necessary conditions in order that the functions F and G satisfy Eqs.(1) through (5) independently of x. Apparently, there is no set of (l, m, n) that satisfies all of the above relationships. In order to solve the problem, we now need to cancel at least one of them. In our previous study (3) we found that the second buoyancy term, i.e. [G2] in Eq.(2), is negligibly small compared to the other terms. This is a feasible approximation in a range of sloping angle θ realized in lakes and reservoirs. It was confirmed from the authors' order argument that $o[G2] << o[G1]$ in a wide range of θ. This will be verified later by comparing the theory and the experiment.

Now, the exponents are finally determined by neglecting [G2] in Eq.(2) as

$$l=1/4, \quad m=3/4, \quad n=0 \tag{8}$$

In contrast, the exponents are as follows in the case when a "constant and uniform buoyancy flux" is imposed on the bed , which have been obtained in the authors' previous study (3).

$$l=1/5, \quad m=4/5, \quad n=1/5 \tag{9}$$

Substitution of Eqs.(6) and (8) into Eqs.(2) and (3) leads to the following ordinary differential equations.

$$\frac{1}{2}F'^{2} - \frac{3}{4}FF'' - G - \Pr F''' = 0 \tag{10}$$

($\Pr \equiv \nu / \kappa_T$: Prandtl number)

$$\frac{3}{4}FG' + G'' = 0 \tag{11}$$

The problem now is to solve $F(\eta)$ and $G(\eta)$ under given boundary conditions. The equations' forms are the same as those formulated by Schlichting (3).

The boundary conditions Eqs.(4) and (5) are then rewritten as

$$F(0)=F'(0)=0, \quad G(0)=1, \quad F'(\infty)=0, \quad G'(\infty)=0 \quad . \tag{12}$$

In these formulations, the proportional coefficients (a, b, e) are defined as follows so that the equation system is described in simplified functional forms as shown later.

$$a = \left(\kappa_C^{-2} C_b \beta g \sin\theta\right)^{-1/4}, \quad b = \left(\kappa_C^{2} C_b \beta g \sin\theta\right)^{1/4}, \quad e = C_b$$

Then the variables in Eq.(6) are rewritten as

$$\eta = (\kappa_C^{-2} C_b \beta g \sin\theta)^{1/4} z x^{-1/4} \tag{13}$$

$$\psi = (\kappa_C^{2} C_b \beta g \sin\theta)^{1/4} x^{3/4} F(\eta) \tag{14}$$

$$C = C_b G(\eta) \quad . \tag{15}$$

Once $G(\eta)$ is solved, the solute flux at the sloping boundary can be computed from the following equation .

$$F_C = -\kappa_C \left.\frac{\partial C}{\partial z}\right|_{z=0} = -G'(0)(\kappa_C^{2} C_b^{5} \beta g \sin\theta)^{\frac{1}{4}} x^{-\frac{1}{4}} \tag{16}$$

Normalization

Assuming the reference scale of solute concentration to be C_0=C_b, the velocity and length scales can be defined so that they satisfy the following equations.

$$P_e \equiv \frac{U_0 L_0}{\kappa_C} = 1, \quad U_0 C_0 = U_0 C_b = F_{C0} \tag{17}$$

(L_0, U_0, F_{C0}) are now

$$\left.\begin{aligned} L_0 &= (\kappa_C^{-2} C_b \beta g \sin\theta)^{-1/3} \\ U_0 &= (\kappa_C C_b \beta g \sin\theta)^{1/3} \\ F_{C0} &= (\kappa_C C_b^{4} \beta g \sin\theta)^{1/3} \end{aligned}\right\} \tag{18}$$

Eqs.(13) through (16) are eventually normalized in terms of the reference scales as follows:

[Dependent variables] $\eta = \tilde{z}\tilde{x}^{-1/4}, \quad (\tilde{x}, \tilde{z}) \equiv (x / L_0, z / L_0)$ (19)

[Velocity components] $\tilde{u} \equiv u / U_0 = \tilde{x}^{1/2} F'(\eta)$ (20)

$\tilde{w} \equiv w / U_0 = \tilde{x}^{-1/4} \{\eta F'(\eta) - 3F(\eta)\} / 4$ (21)

[Concentration] $\tilde{C} \equiv C / C_0 = G(\eta)$ (22)

[Solute flux at the bed surface] $\tilde{F}_C \equiv F_C / F_{C0} = -\tilde{x}^{-1/4} G'(0)$ (23)

Solutions

Solutions for $F(\eta)$ and $G(\eta)$ are obtained by integrating Eqs.(10) and (11) under the boundary conditions Eq.(12). The numerical integration was conducted by using the so-called "quasi-linearization". Fig.2 shows solutions for the x-wise velocity component $F'(\eta) = \tilde{u} \cdot \tilde{x}^{-1/2}$ and the solute concentration $G(\eta) = \tilde{C}$. Fluid diffusivity and viscosity are κ_T=0.0014 cm^2/s and ν=0.013cm^2/s for the water temperature of 10℃ and the corresponding Prandtl number Pr is about 9.0. Dependency of the solutions on Pr is also shown in the figure.

Non-dimensional solutions for the streamline $\tilde{\psi} \equiv \psi / (U_0 L_0) = \psi / \kappa_C$, the concentration $\tilde{C}$ and the velocity in x-direction $\tilde{u}(\tilde{z})$ are plotted on the $(\tilde{x}, \tilde{z})$-plane in Fig.3.

Here, a layer thickness of the plume δ is defined as the vertical distance from the wall z at which the concentration takes 5% fraction of that at the bed surface C_b, i.e. $C=0.05C_b$ at $z=\delta$. It should be noted that there is little difference of the power law dependency of δ on x for different values of concentration fraction in a range between 0.02-0.20. Therefore, the fraction 0.05 might be a good measure of defining layer thickness from the concentration profiles. Considering $C/C_b=G(\eta=\eta_S=5.3)=0.05$ from the solution in Fig.2(a) and Eq.(19), a functional dependency of the layer thickness $\tilde{\delta} \equiv \delta / L_0$ at the distance $\tilde{x}$ is obtained as

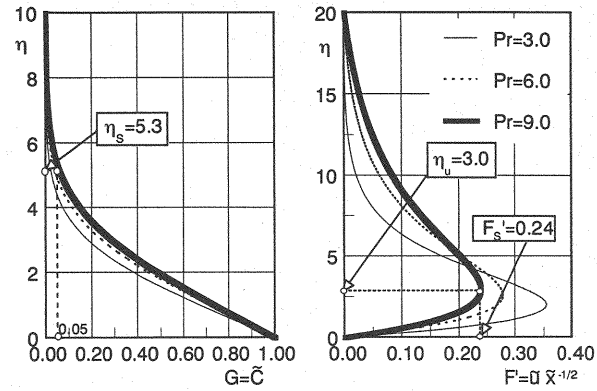

(a) Concentration, $G(\eta) = \tilde{C}$ (b) Velocity, $F'(\eta) = \tilde{u} \cdot \tilde{x}^{-1/2}$

Fig.2 Solutions of concentration and velocity, $G(\eta)$ and $F'(\eta)$

$$\tilde{\delta} = \eta_S \cdot \tilde{x}^{1/4} = 5.3\tilde{x}^{1/4} . \tag{24}$$

The maximum velocity U_{max} is deduced from Fig.2(b) and Eq.(20) in the same manner as $\tilde{\delta}$ as a function of $\tilde{x}$ as

$$\tilde{U}_{max} = F_S' \cdot \tilde{x}^{1/2} = 0.24\tilde{x}^{1/2} . \tag{25}$$

Longitudinal variation of solute flux from the bed surface is obtained as

$$\tilde{F}_C = 0.27\tilde{x}^{-1/4} \tag{26}$$

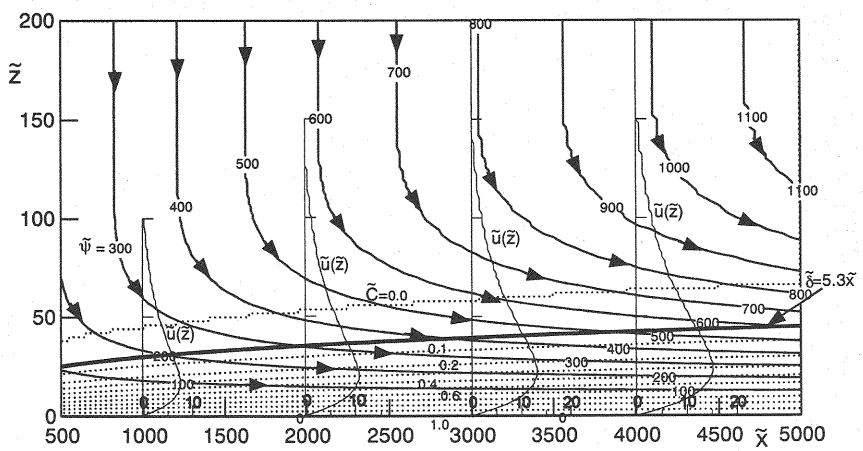

Fig.3 Dimensionless solutions of streamlines $\tilde{\psi}$, concentration $\tilde{C}$ and horizontal velocity $\tilde{u}(\tilde{z})$

after substituting the solution $G'(0)$=-0.27 into Eq.(23).

On the other hand, the concentration or buoyancy is kept constant independently of $\tilde{x}$ as seen in Eq.(22).

The longitudinal evolution of the layer thickness described by Eq.(24) is caused by entrainment of ambient fluid into the plume. This increases solute transport in the x-direction, too. The solute flux increase in the longitudinal direction is evaluated from Eqs.(24) and (25) as

$$\int_0^\infty \tilde{u}\tilde{C}d\tilde{z} \approx \tilde{U}_{\max}\tilde{C}\tilde{\delta} \propto \tilde{x}^{1/2}\tilde{x}^{0}\tilde{x}^{1/4} \propto \tilde{x}^{3/4} \quad . \tag{27}$$

Eq.(27) and conservation of solute concentration lead to the following functional dependency of $\tilde{F}_C$ on $\tilde{x}$.

$$\tilde{F}_C \approx \tilde{w}\tilde{C}\Big|_0 \approx -\frac{\partial}{\partial x}\int_0^\infty \tilde{u}\tilde{C}d\tilde{z} \propto \tilde{x}^{-1/4} \tag{28}$$

This is consistent with Eq.(26).

EXPERIMENT

For the convenience of experimental instrumentation, the laboratory experiment was carried out in respect to a thermal plume system instead of a solute plume system. One of the reasons for doing this is that it is much easier to supply a uniform buoyancy flux by heating up a sloping plate rather than by uniformly discharging solute-buoyant-water such as salt water from a sloping permeable bed. The other advantage of using the thermal plume is that a multi-point measurement is easier and inexpensive in a temperature field than in a concentration field. In order to maintain hydrodynamic similarity between the thermal and solute plume systems, the experimental setup in Fig.4 should be the vertically reversal of the original system in Fig.1. The two plume systems are dynamically identified with each other by interpreting buoyancy as $\alpha T \Leftrightarrow \beta C$, where α is a thermal expansion coefficient and T is water temperature. A detailed description of the experimental facility can be found in the authors' previous papers (3, 5).

The two parameters, that is, the sloping angle θ and the surface temperature T_b of the heating plate, were varied in the experiment. The experiment was conducted with θ=15, 30, 45, 60, 75° and T_0 (=T_b)=3.6~9.7℃. A relay circuit and a PC controller were used in order to regulate the heating plate to keep it at a constant temperature T_0. Water temperature was measured by thermocouples at 6 cross sections in the x-direction. The temperature profile was obtained from 20 points measurements in the z-direction at each cross section. The temperature was monitored after switching on the heater in order to watch if the plume motion came to a steady state. After confirming that there was no more temporal variation in temperature field, image and data recording were started. It usually takes ten to twenty minutes until the plume becomes a steady one.

Since the fluid motion is very slow and the fluid density is inhomogeneous, it is not so easy to measure flow velocity by using sensor probes. A combination of suitable flow visualization and image processing technique might give better results than conventional probe measurements in this system. However, a very fine tracer particle that is scarcely influenced by buoyancy is required in the flow visualization to obtain high tracing performance. The particle used in this study is a micro nylon particle with a diameter ranging between 10 to 50μm. Even for such a small diameter, most of the particles had already settled down before taking the measurement. Nevertheless, the rest of the particles were still left in suspension in the next few hours which were utilized for tracing fluid

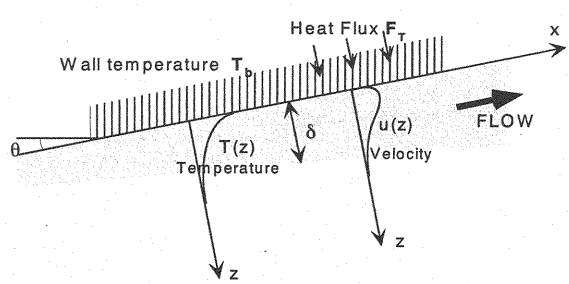

Fig.4 Experimental model

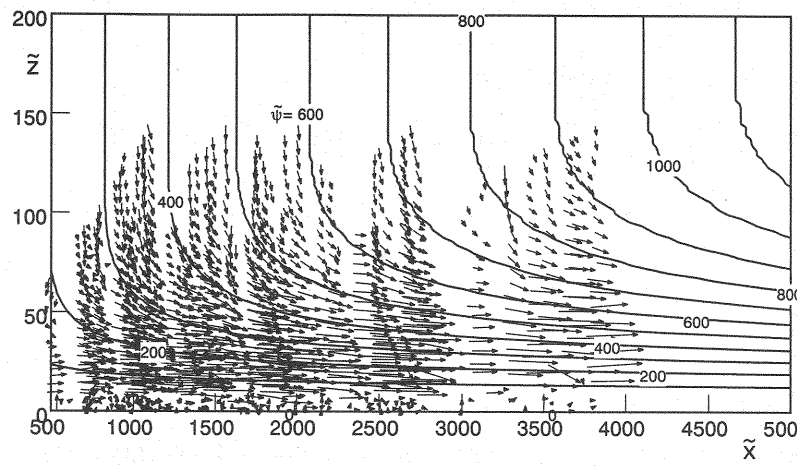

Fig.5 Normalized velocity vectors from the PTV measurement compared with theoretical streamlines in the $(\tilde{x}, \tilde{z})$ plane.

motions. Assuming the suspension duration of the rest particles to be one hour and the settling distance to be 0.5m, the settling velocity was estimated to be o(0.01cm/sec). Since this is negligibly small compared to the plume velocity, o(1.0cm/sec), the particle's tracing performance is thought to be scarcely influenced by particle settling even in such a sluggish flow. In addition, specific density difference of the thermal plume is typically $o(10^{-5}\sim10^{-7})$ which is much smaller than specific density difference between the particle and the ambient water, $o(10^{-2})$. Therefore, it was concluded that the plume's buoyancy has little influence on tracer particles' behaviors. A x-z plane of the test section was illuminated by a laser light sheet. The image processing used here is a so-called "particle tracking velocimetry, PTV", which is a method of computing local flow velocity from trajectory of tracer particles. The PTV computer program is an original code developed by the authors, which is referred in our previous papers (6). The present velocimetry will be carefully examined and verified by comparing the experimental data with the theoretical solutions. This will be discussed later.

The maximum velocity and the layer thickness were typically in the order of U_{max}=1cm/s and δ=1cm, respectively, and the corresponding Reynolds number was of the order of several hundreds.

VELOCITY AND BUOYANCY PROFILES

Velocity

Fig.5 shows normalized velocity vectors $(\tilde{u}, \tilde{w})$ collected from all the cases and plotted in the $(\tilde{x}, \tilde{z})$ plane. The vectors are ensemble averages from instantaneous values over a mesh size of 1mm×50mm. They are compared with the theoretical streamline $\tilde{\psi}$ represented by solid lines. The theory describes accurately the plume's behaviors such as entrainment of ambient fluids into the plume, plume layer evolution and acceleration in the longitudinal direction and so on.

Temperature (Buoyancy)

An example of temperature isopleths is presented with

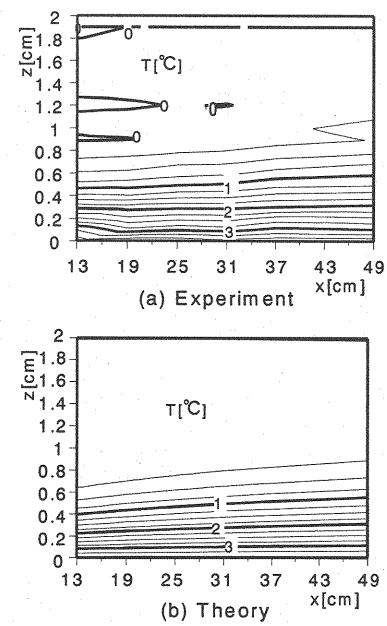

Fig.6 Temperature profiles for the case of (θ=15°, T_0=3.6℃).

the theory in Fig.6. A satisfactory agreement between them is confirmed.

Velocity Profiles in Self-Similar Functional Forms

The velocity vectors collected from all the experimental cases are normalized as in Eqs.(20) and (21) , i.e.

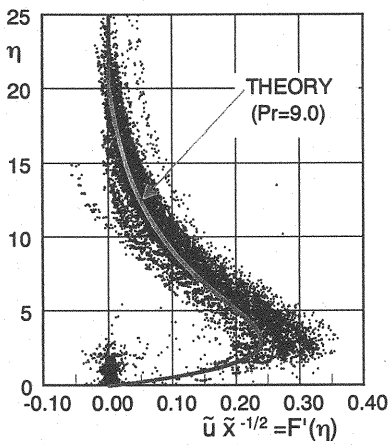

Fig.7 Velocity component in the x-direction in a self-similar functional form $\tilde{u}\cdot\tilde{x}^{-1/2}$ with the theoretical solution $F'(\eta)$.

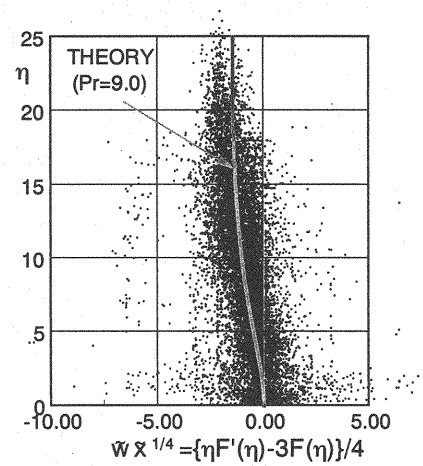

Fig.8 Velocity component in the z-direction in a self-similar functional form $\tilde{w}\cdot\tilde{x}^{1/4}$ with the theoretical solution $\{\eta F'(\eta) - 3F(\eta)\}/4$.

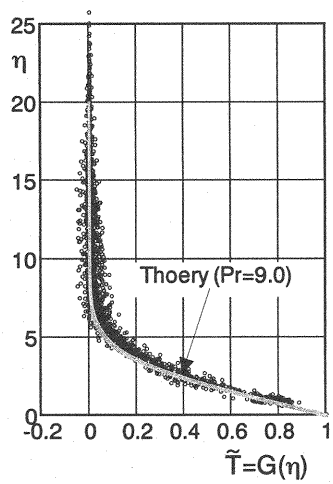

Fig.9 Self-similar profile of buoyancy. Circles are the experiment and the solid curve is the theoretical solution as in Eq.(32).

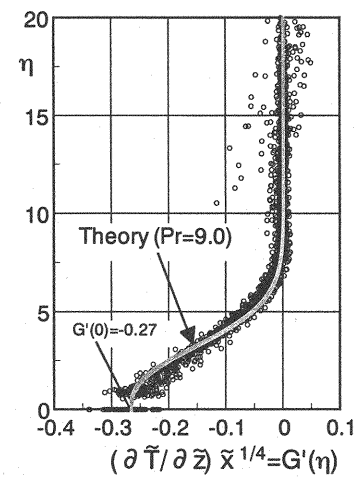

Fig.10 Buoyancy gradient corresponding to Fig.9. Definition is in Eq.(33). The solution at the bottom $G'(0)$=-0.27 provides dimensionless buoyancy flux from the bed surface.

$$\tilde{u} \cdot \tilde{x}^{-1/2} \equiv (u / U_0)(x / L_0)^{-1/2} \tag{29}$$

$$\tilde{w} \cdot \tilde{x}^{1/4} \equiv (w / U_0)(x / L_0)^{1/4} \tag{30}$$

and compared with their theoretical solutions given in Figs.7 and 8, respectively.

$$F'(\eta), \quad \{\eta F'(\eta) - 3F(\eta)\} / 4 \tag{31}$$

The plotted data points are correlated well with the theoretical curves. In Fig.7, however, some data points are concentrated around $F'(\eta) = 0$ in the range of $0<\eta<2$, which may be caused by an error made in identifying the origin of the vertical coordinate, i.e. z=0. It can reduce the error by clearly marking the wall surface so that the origin could be accurately identified from the image. Apart from this, the experimental data points are well fitting with the theoretical curves.

Buoyancy Profile in a Self-Similar Functional Form

Replacing concentration C with temperature T as $\alpha T \Leftrightarrow \beta C$, the normalized thermal buoyancy from the experiment $\tilde{T} \equiv T / T_0$ is compared with the solution as

$$\tilde{T} \equiv T / T_0 = G(\eta) \ . \tag{32}$$

The normalized thermal buoyancy $\tilde{T}$ collected from all the measuring points for all the experiments are plotted in Fig.9, which agree closely with the self-similar solution $G(\eta)$ shown by the solid curve. The following solution for the dimensionless buoyancy gradient is also shown in Fig.10.

$$(\frac{\partial \tilde{T}}{\partial \tilde{z}})\tilde{x}^{\frac{1}{4}} \equiv (\frac{\partial T}{\partial z})(\frac{L_0}{T_0})(\frac{x}{L_0})^{\frac{1}{4}} = G'(\eta) \tag{33}$$

Here, it should be noted that the buoyancy flux from the bed surface is given by the solution $G'(0)$=-0.27 and this is verified by the measurement as seen in the figure. The longitudinal development of the dimensionless buoyancy flux $\tilde{F}_C$ is then given by Eq.(26) which was discussed in the previous section.

PLUME PROPERTIES

Development in the Longitudinal Direction

The longitudinal development of the plume can be discussed based on the analysis given in the Section 2.3. The layer thickness δ, the maximum horizontal velocity U_{max} and the buoyancy flux F_C from the bed surface are shown as functions of x in

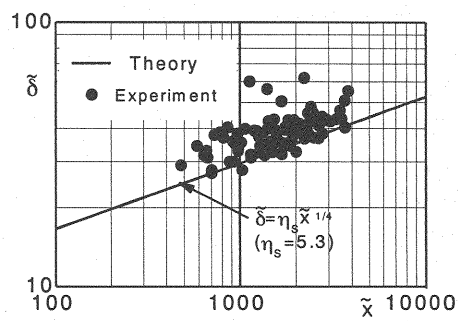

Fig.11 Layer thickness δ against longitudinal distance x.

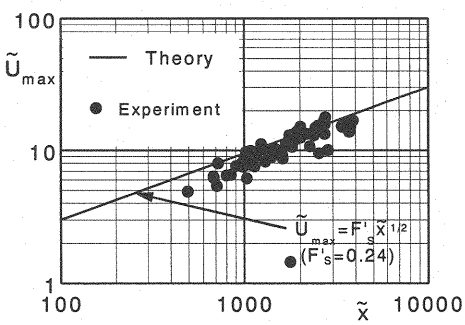

Fig.12 Maximum velocity U_{max} against longitudinal distance x.

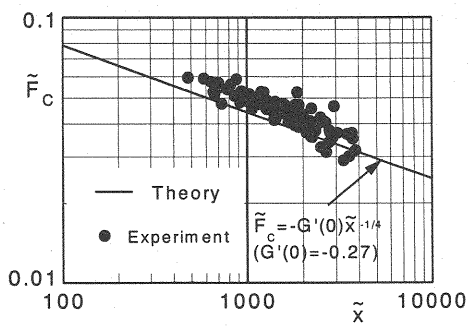

Fig.13 Buoyancy flux from the bed surface F_C against longitudinal distance x.

Fig.11, 12 and 13, respectively. The experimental data are normalized and plotted in solid circles and compared with the theoretical curves given by Eqs.(24), (25) and (26). The solutions slightly overestimate δ and F_C, while U_{max} is somewhat underestimated. Nevertheless, their functional dependencies on the longitudinal distance agree closely with the theoretical power laws. This means that the flow structure is kept self-similar in the course of its longitudinal development.

Effects of Sloping Angle θ and Bed Surface Temperature $T_0(=T_b)$ on the Plume Properties

Figs.14, 15 and 16 represent the effects of angle and surface temperature of the sloping boundary (θ, T_0) on the plume's properties (δ, U_{max}, F_C). The ordinate in each diagram is normalized by a reference value from the experimental case of θ=45°, T_0=9.7℃ noted with the subscript "s". The theoretical curves agree fairly well with the experimental data. The functional dependencies of the plume's properties on x are summarized in Table 1.

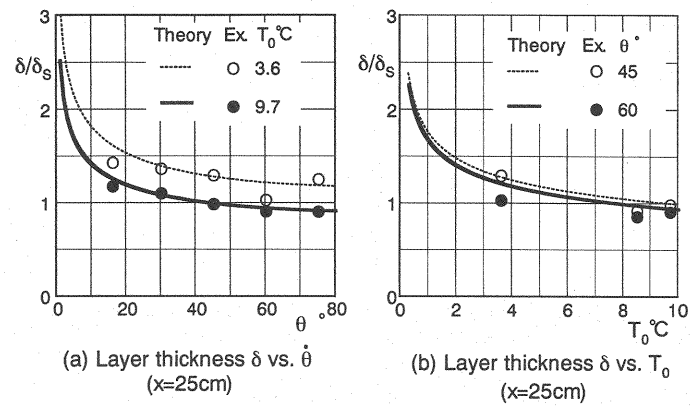

Fig.14 Plume's layer thickness δ dependent on (θ, T_0).

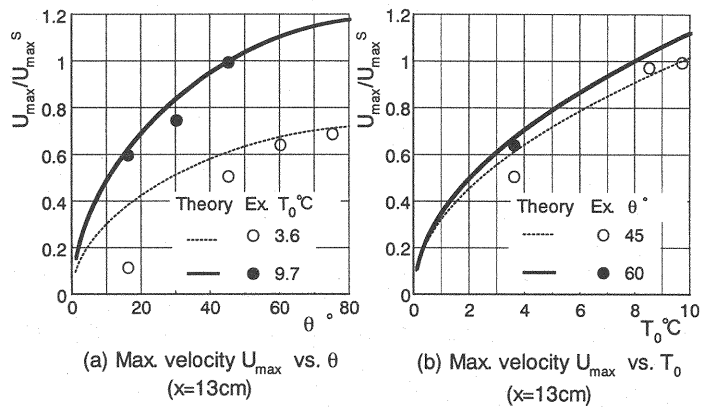

Fig.15 The maximum fluid velocity U_{max} dependent on (θ, T_0).

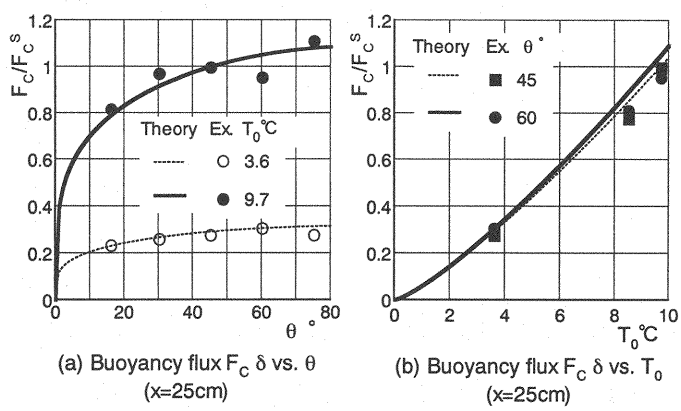

Fig.16 Buoyancy flux F_C dependent on (θ, T_0).

CONCLUDING REMARKS

Due to reduction in an anaerobic hypolimnion in eutrophic reservoirs, a large amount of ionic metals and inorganic nutrients are released from the "sediment-water" interface. This is responsible for contamination of hypolimnetic water. On an inclined bed the released solutes generate a plume along

Table 1 Dependency of the plume's properties (δ, U_{max}, F_C) on the sloping angle θ and the bed surface temperature T_0. "+" and "-" mean a positive and negative correlation between the variables, respectively.

Parameters \ Variables	Layer thickness δ	The maximum velocity U_{max}	Buoyancy flux from the bed F_C
Slope angle θ	−	+	+
Wall temperature T_0	−	+	+

the sloping bed because of its extra density, which transports the contaminated water down to the bottom of the reservoir.

In the present study a simplified plume model is designed to examine its flow structure, buoyancy field and scalar transport. The experimental setup is such that a thermal plume is generated along an inclined sloping plate whose surface is heated at a constant temperature. This is hydrodynamically equivalent to a solute plume system produced in a prototype reservoir. Theoretical solutions for velocity and buoyancy are obtained by conducting a self-similar flow analysis. The solutions agree quite well with the experiment in respect to velocity, buoyancy and the plume's development in the longitudinal direction.

From the analysis, we can estimate transport rate, the concentration and releasing flux of dissolved components under given sloping angles and solute concentration on the bed. The present solution could be a sub-model which is a part of a dynamic reservoir model by which water quality could be predicted more precisely. Further field data are required, however, for satisfying the requirement of an efficient water quality model, such as solute concentration on the bed boundary, diffusivity of released dissolved components, transport coefficient at the sediment-water interface, etc..

ACKNOLEDGEMENTS

The present research was financially supported by the Grant in Aid for Scientific Research, Basic Research (B) (2), from the Japan Ministry of Education, Grant No. 12555148, Project Leader; Kohji Michioku.

REFERENCES

1. Michioku,K., Kanda,T. and Nakamura,A.: Thermohaline convection in a eutrophic reservoir with an inverse thermal stratification, 4th Symposium on Environmental Fluid Mechanics, pp.439-440, 1999 (in Japanese).
2. Schlichting,H.: *Boundary-Layer Theory*, 6th Ed., McGraw-Hill, pp.253-310, 1968.
3. Michioku,K., Matsushita,K. and Takahashi,T.: An experiment and an analysis on inclined plume generated by salinity flux supplied from a sloping bed, Proc. JSCE, No.649/II-51, pp.49-60, 2000(in Japanese).
4. Fukushima,Y.: Analysis of inclined wall plume by turbulence model, Proc. JSCE, No.399/II-10, pp.65-74, 1988 (in Japanese).
5. Michioku,K., Fujita,I., Takahashi,T. and Yabumoto,K.: PTV of an inclined plume generated by uniform buoyancy flux on a sloping wall, Flow Visualization, Journal of the Visualization Society of Japan, Vol.20, Suppl. No.1, pp.91-94, 2000 (in Japanese).
6. Fujita,I. and Toomatsu,A.: Velocity measurement of open channel turbulent flow by using image processing , J. Applied Mechanics JSCE, Vol.1, pp.627-636, 1999.

APPENDIX – NOTATION

The following symbols are used in this paper:

$B(x, z)$ = buoyancy;

$C(x, z)$ = solute concentration;

C_b = solute concentration at the bed surface;

F_C = solute flux at the bed surface;

$F(\eta)$, $G(\eta)$ = dimensionless self-similar functions corresponding to ψ and C, respectively;

g = gravitational acceleration;

p = pressure;

P_e = Peclet number;

T_b = temperature at the bed surface;

(u, w) = flow velocity components in the (x, z) directions;

U_{max} = the maximum of u at a cross-section x;

$\sim$ = a normalized version of a variable;

(x, z) = space coordinates in the directions along and perpendicular to the sloping boundary;

β = a proportional coefficient between buoyancy and concentration C;

δ = plume layer thickness;

$\eta = azx^{-l}$ = a dependent variable in a self-similar function system;

η_S = a value of η for which $G(\eta)=0.05$;

θ = sloping angle of the inclined boundary;

κ_C = molecular diffusivity a solute substance;

ν = kinematic viscosity; and

$\psi(x, z)$ = a stream function.

(Received September 12, 2001 ; revised January 11, 2002)